ISSN 1995-0780, Nanotechnologies in Russia, 2020, Vol. 15, Nos. 3–6, pp. 326–332. © Pleiades Publishing, Ltd., 2020.
Russian Text © The Author(s), 2020, published in Rossiiskie Nanotekhnologii, 2020, Vol. 15, No. 3, pp. 337–343.

DEVICES AND PRODUCTS BASED ON NANOMATERIALS AND NANOTECHNOLOGIES

Model Study of a Cold Start of a Power Plant Based on a Polymer Electrolyte Membrane Fuel Cells in the Conditions of Arctic Temperatures

G. N. Voloshchenko[a], A. A. Zasypkina[a,*], and D. D. Spasov[a,b]

[a] *National Research Center Kurchatov Institute, Moscow, 117556 Russia*

[b] *National Research University Moscow Power Engineering Institute, Moscow, 111250 Russia*

**e-mail: adelinazasypkina@yandex.ru*

Received June 9, 2020; revised July 27, 2020; accepted July 27, 2020

Abstract—A model calculation of the startup of a power plant based on a polymer electrolyte membrane fuel cell (PEMFC). The power plant is equipped with a recombiner with a nanostructured hydrogen oxidation catalyst and a bubbler, filled with methanol, which absorbs water vapor, drying the heated air to prevent ice formation inside the fuel cell, which allows for autonomous cold start and operation in the Arctic region. A mathematical model was developed of start-up of PEMFC capacity 1 kW from ambient temperature in the Arctic region to the operating temperature of the fuel cell (warming up from −50 to +50°C). The characteristics of the heating modes were determined for the gradients of the fuel cell heating rate from 0.1 to 0.5°C/s. The proposed scheme of the heating unit and the mode of starting the power plant make it possible to reduce the heating element heating time to the operating temperature to ~6 min, as well as to reduce the volume of the heating unit used and to reduce the consumption of hydrogen supplied in a mixture with air to 3 vol %. The proposed scenario of cold start ensures the temperature stability of the heating unit, which guarantees the safety of heating the fuel cell and the installation as a whole. The use of methanol to remove water vapor from the hydrogen stream and replace them with methanol vapor allows the cold start temperature of the fuel cell to be reduced to -50°C due to the prevention of crystallization of water vapor in the bulk of FC components at the initial stages of heating.

DOI: 10.1134/S1995078020030155

INTRODUCTION

The problem of energy supply to the Far North and the Arctic under conditions of sharply negative temperatures and underdeveloped infrastructure, is urgent. A promising and modern solution to this problem is the introduction of environmentally friendly and efficient energy generation technologies, in particular technologies based on the use of proton exchange membrane fuel cells (PEMFC). PEM fuel cells operate in ambient temperature ranges from −20 to +50°C without additional energy supply [1], but starting them at sharply negative, arctic temperatures up to −50°C is a challenge.

Investigations into the operation of fuel cells at low temperatures began long ago [2–6]. There have been practical advances in starting PEMFC in the temperature range from −20 to −15°C [7–10]. However, no optimal solution to the problem of cold start-up of power supply systems with PEM fuel cells has been found, which indicates the relevance of additional research in this area [11–13].

Cold start strategies for PEMFC-based power plants can be divided into two groups. The first uses an external heating source to generate heat and delivering it to the fuel cell through the coolant [14, 15]. The methods used in this case are effective from the point of view of launch time [8, 16–19]. Thus, in [16, 17] no more than 5 min was spent on ice melting in the fuel cell, in [18] the fuel cell was heated to 60°C in 40 min, and in [19], the fuel cell was heated from −10°C to a rated power of 1.2 kW in 22 minutes. In this case, reagent gases were used as a coolant. However, the addition of an external heater and additional heating fluids affects the volume, weight, cost and energy efficiency of similar PEMFC-based installations. For example, in [15], the presence of an external heater connected to the output of the FC battery leads to a significant increase in hydrogen consumption during the operation of the installation by an average of 50%.

The second group of strategies implies self-heating of the fuel cell during a cold start, which is based on a purge procedure during shutdown to prevent water accumulation, or by cleaning with antifreeze substances, for example, a water-methanol solution [20]. Also, internal heating during start-up is carried out using the heat generated during exothermic hydrogen

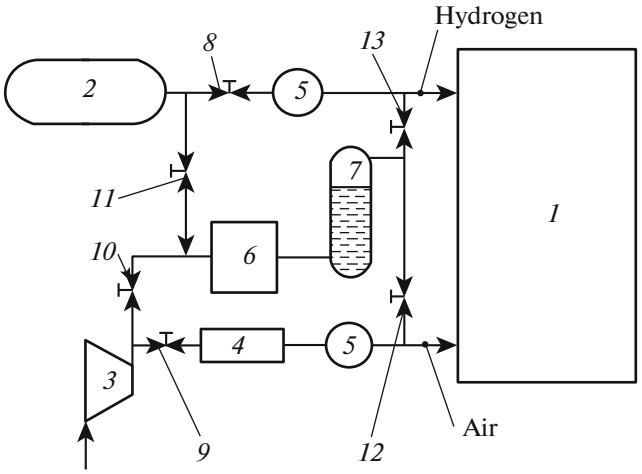

Fig. 1. Scheme of a power plant with PEMFC for the Arctic regions: (*1*) fuel cell, (*2*) a container with hydrogen, (*3*) blower, (*4*) humidifier, (*5*) pressure regulator, (*6*) heating unit (catalytic recombiner), (*7*) bubbler, (*8–13*) metering valve.

oxidation reaction. So, a diluted mixture of hydrogen in air is fed into the air supply channel of the plant based on FC, presented in [21], and due to the exothermic reaction of hydrogen with oxygen, FC self-heating to the operating temperature occurs. Here, the disadvantage is the lack of the possibility of autonomous start of the power plant in low temperatures more than –5°C, since the heat from the oxidation reaction in the case of limiting the hydrogen concentration is not enough to heat the fuel cell and prevent freezing of water vapor, and an increase in hydrogen concentration can lead to direct damage to the FC, for example, destruction of the membrane as a result of overheating. Study of a power plant using PEMFC has been conducted [22], which provides for the possibility of cold start, in which starting heating should occur due to the heat released during the recombination of hydrogen and oxygen on the surface of the electrodes. However, at Arctic temperatures, the resulting water immediately forms an ice film on the surface of the electrodes and, therefore, blocks the further recombination process.

In [23], an adaptive strategy of internal self-heating with the help of heat generated by fuel cells in a galvanostatic mode is proposed. Cold start is carried out on the basis of purging the PEMFC reagents when disconnecting and heating the FC at startup. The melting point of water was reached in almost 50 s, with an energy consumption of 201.7 J/cm^2.

At the moment, fuel cells that operate under low-temperature conditions are known that use direct oxidation of methanol [24, 25], but these have a number of disadvantages, such as increased weight and size characteristics, low power characteristics, and loss of the reagent due to diffusion through the membrane. At the same time, the existing scientific and technical groundwork in the field of fuel cells with direct oxidation of alcohols [26–28] makes it possible to count on the successful use of this reagent as part of a power system based on hydrogen-air PEM fuel cells, which ensures the possibility of their efficient operation at temperatures below –50°C. Earlier studies on start-up in fuel cells have been only carried out for temperatures as low as –20°C [8, 20, 22, 23, 29–31], which is not sufficient for the Arctic zone.

The purpose of this work was to simulate an autonomous cold start of a power plant based on PEMFC under conditions of Arctic temperatures up to –50°C without using additional heat sources. To reduce cold start temperature, it is proposed to use methanol as antifreeze for fuel cell and to dry reagent gases in the investigated power plant based on PEM fuel cell. The developed method of launching the installation in the Far North, implemented in the form of a dynamic model of the launch mode, will also allow the main parameters of the power plant operation to be optimized.

NUMERICAL SIMULATION

Schematic diagram of the power plant. The development of a mathematical model of the start-up mode of PEM fuel cell at negative ambient temperatures was carried out for a power plant, the schematic diagram of which is shown in Fig. 1.

The power plant contains PEMFC (*1*), a catalytic recombiner (*6*), a bubbler (*7*), hydrogen sources (*2*) and air (*3*), a humidifier (*4*), and pressure regulators (*5*). It works as follows. Hydrogen from a hydrogen source (*2*) and air from the blower (*3*) in a given proportion are fed to the catalytic recombiner (*6*), where they interact with the release of heat and the formation of water vapor. For this recombiner, the nanocatalyst described in [32] can be used. In this case, the loading of the platinum will be approximately 0.4 mg/cm^2. The active platinum surface for this nanocatalyst is about 50 m^2/g. The resulting heated mixture enters the bubbler (*7*), filled with methanol, which absorbs water vapor, drying the heated air. The use of methanol as an air dryer that heats the fuel cell makes it possible to significantly reduce the temperature of starting the fuel cell because the absence of water vapor prevents the formation of an ice crust on the surface of the electrodes. It should be noted that starting at such low temperatures is also possible due to the freezing of methanol at –97.6°C. Then the dried heated air enters the anode and cathode spaces of the FC, gradually heating it. After a certain period of time, the increasing temperature of the fuel cell and the entire power plant as a whole reaches a level at which a current-forming reaction is possible. Therefore when the fuel cell temperature reached +10°C, the flow of reagents from the heating unit is directed, bypassing the bubbler directly

into the fuel cell. There was no need to absorb water vapor, since this temperature is sufficient to prevent freezing of water vapor in the volume of the components of the membrane-electrode blocks of the FC. Hydrogen and air begin to be supplied directly to the anode and cathode spaces of the FC, and a voltage and FC starts to work. The heat released at the same time maintains the achieved positive temperature of the power plant. The power plant is protected by the RF patent [33].

The introduction of methanol into the flow of reagent gases, and, therefore, into the nanostructured catalytic layer of the FC, requires the introduction of additional components into the composition of the nanoelectrocatalysts for its efficient oxidation without a drop in the electrochemical characteristics of the FC. In this work, this problem was solved by using hybrid electrocatalysts with $Pt–SnO_2$ nanoclusters, exhibiting high activity in the oxidation reaction of alcohols [34].

Launch model of the plant with PEMFC. The calculations were carried out for a power plant based on a FC battery with a power of 1 kW. The cold start was carried out at an ambient temperature of –50°C, the installation was heated up to the operating temperature of the FC, equal to +50°C. The characteristics of the heating modes were determined for the fuel cell heating rate gradients from 0.1 to 0.5°C/s.

The calculation of the dynamics of heating the power plant begins with the heating unit:

$$dT_{HU} = \frac{(Q_{H_2} - (T_{HU} - T_0)Cp_{reag}G_{input}dt)}{Cp_{GDL}}, \quad (1)$$

where dT_{HU} is the increase in the temperature of the heating unit during dt:

$$dt = \frac{L_{GDL}}{V_{input}}, \quad (2)$$

L_{GDL} is the length of the gas diffusion layer (GDL) with catalyst, V_{input} is the input flow rate of reactants along the GDL with a catalyst:

$$V_{input} = \frac{8.205G_{input}T_0}{\Delta_{GDL}}, \quad (3)$$

G_{input} is the consumption of the input mixture of reagents, T_{HU} is the current temperature of the heating unit, Δ_{GDL} is the gap between adjacent GDL with a catalyst, Cp_{reag} is the average molar heat capacity of the reagent mixture, Cp_{GDL} is the heat capacity of GDL with catalyst, T_0 is the ambient temperature, t is the current time, and Q_{H_2} is the heat of hydrogen oxidation during the time dt:

$$Q_{H_2} = G_{minH_2}dt \times 242\,000, \quad (4)$$

where G_{minH_2} is the minimum hydrogen consumption:

$$G_{minH_2} = L_{GDL}i_{kat0} \times 0.00001036, \quad (5)$$

i_{kat0} is the effective current density of hydrogen oxidation.

As a result of the calculation, the specific heat power of 1 cm of the width of the duct between two GDL with a catalyst was determined:

$$NQ_{reag} = (T_{HU} - T_0)Cp_{reag}G_{input}. \quad (6)$$

Having calculated the thermal power required for heating the fuel cell, according to the formula

$$N_{heatFC} = N_{FC}kQ_{FC}GradT_{FC}, \quad (7)$$

where N_{FC} is the power of FC with SPE, kQ_{FC} is the specific heat of PEMFC, $GradT_{FC}$ is the permissible gradient of heating rate of PEMFC, we determine the required width of the heating unit duct:

$$W_{HU} = \frac{N_{heatFC} + N_{heatM}}{NQ_{reag}}, \quad (8)$$

where N_{heatM} Is the heating power of methanol in the bubbler, calculated as

$$N_{heatM} = G_MCp_MGradT_{FC}, \quad (9)$$

G_M is the amount of methanol, Cp_M is the specific heat of methanol.

The amount of methanol was determined by the amount of water formed during the heating of the PEMFC, and was corrected as a result of the cyclic calculation of the heating mode.

The FC temperature was calculated using the formula

$$dT_{FC} = \frac{Cp_{reagEx}G_{output}dT_{HU}W_{HU}(T_{HU} - T_{FC}) + Q_{diss}}{Cp_{FC} + Cp_M}, \quad (10)$$

where Cp_{reagEx} is the heat capacity of the reagent mixture at the outlet from the heating unit, G_{output} is the total consumption of reagents at the exit from the heating unit, Q_{diss} is the heat of dissolution of water in methanol.

In the course of the calculation, the value of the coefficient determining the ratio of hydrogen and oxygen in the inlet mixture of hydrogen and air was also refined in such a way that the final temperature of the heating unit would exceed the final temperature of the fuel cell, which guaranteed heating of the entire installation. This temperature was called the limiting temperature of the heating unit and was defined as the fuel cell heating range (in this case, 100°C), increased by a certain number of degrees (from 10 to 110°C).

RESULTS AND DISCUSSION

The main calculated parameters, namely, heating time, volume of the heating unit, and hydrogen con-

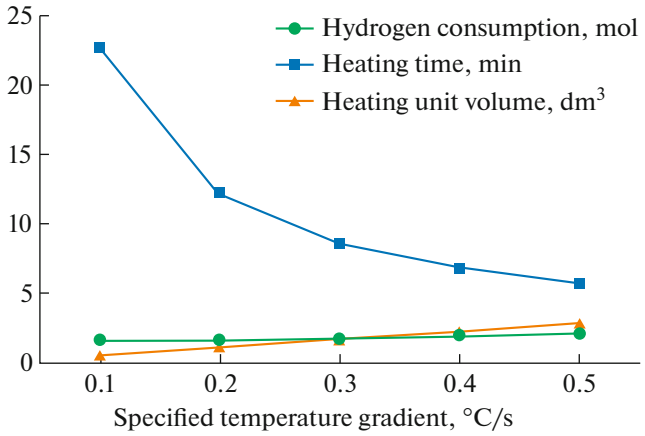

Fig. 2. (Color online) Dependence of the heating time, the volume of the heating unit and the hydrogen consumption on the given gradient of the heating rate of PEMFC.

sumption for heating, depending on the specified temperature gradient of the fuel cell, are shown in Fig. 2. With an increase in the temperature gradient, the heating time decreased, and the volume of the heating unit and the hydrogen consumption increased, which was to be expected. At the same time, the values of the main parameters obtained as a result of calculations indicate the effectiveness of the considered heating method. Indeed, the heating time of the power plant from −50 to +50°C was from 339 to 1362 s, while in [18], the heating time of the fuel cell from −20 to +60°C was approximately 2500 s (42 min). In this case, the hydrogen consumption for heating is equivalent to several minutes of FC operation at the nominal mode, and the volume of the heating unit is comparable with the volume of fuel cell (~0.002 m^3). For example, in [17] an electric heater was used to heat the air, and in [19] a large-sized radiator was used. Note that the mole fraction of hydrogen in a mixture with air supplied to the heating unit is less than 3%, which is below the self-ignition limits and ensures the safety of the entire installation.

Simulation of the proposed scenario of cold start of PEMFC showed the possibility of autonomous heating of the power plant from the ambient temperature of −50°C to the operating temperature of +50°C with the restoration of all electrochemical parameters of the fuel cells to their initial values. The output power of the FC after the cold start scenario in the operating mode will be 0.35 W/cm^2, which will exceed the average values of the electrochemical parameters of world analogues presented in the literature.

The heat balances of the heating mode are shown in Fig. 3. The energy of hydrogen in the heating unit (Fig. 3a) was distributed between the GDL with the catalyst and reagents, and with an increase in the gradient, the share of heat for heating the GDL increased. Thus, at a maximum temperature rise gradient of 0.5°C/s, 73% of the heat was accounted for by heating the reactants and 27% by heating the GDL with the supported catalyst. In turn, the heat of the reagents was distributed between the heating of the fuel cell (67% at 0.5°C/s), methanol (31% at 0.5°C/s), and losses with exhaust gases after the FC (2% at 0.5°C/s). Slow heating of the power plant is preferable because of the decreased heat losses and the reduced volume of the heating unit to a minimum size, while the heating time was only about 20 min. Heat costs for the heating of methanol decreased due to heat release upon absorption of water vapor alcohol, which is also a positive side of the use of methanol, as this effect makes it possible to reduce the energy consumption for heating the fuel cell. In this case, the heat balance depends little on the heating gradient (Fig. 3b).

It is of interest to calculate the change in the temperature of the heating unit at different gradients of the

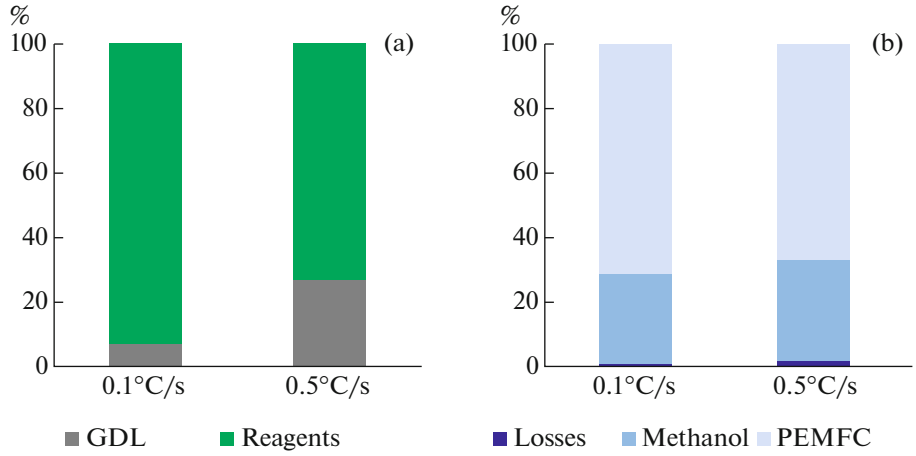

Fig. 3. (Color online) Heat distribution between GDL with supported catalyst and reagents in the heating unit (a) and between PEMFC, methanol, and losses with exhaust gases after FC (b) at heating rate gradients equal to 0.1 and 0.5°C/s.

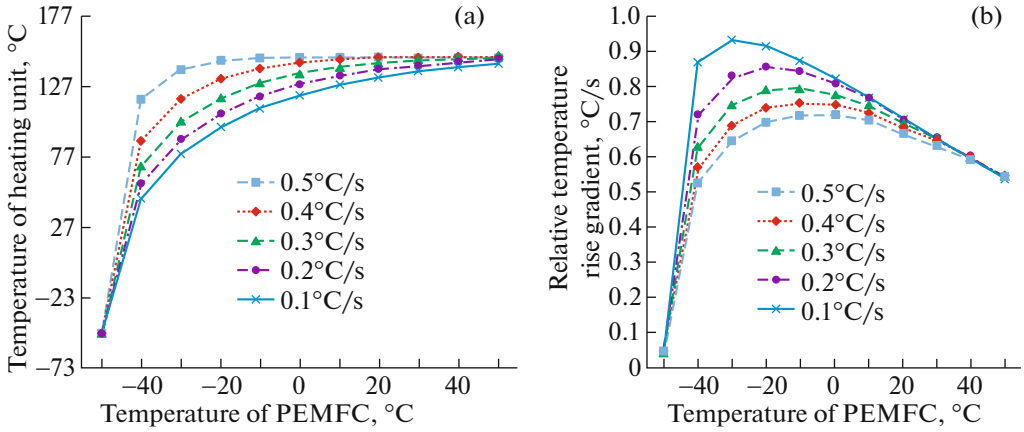

Fig. 4. (Color online) Dependence of the temperature of the heating unit (a) and the relative gradient of temperature rise (b) at different gradients of the heating rate on the FC temperature.

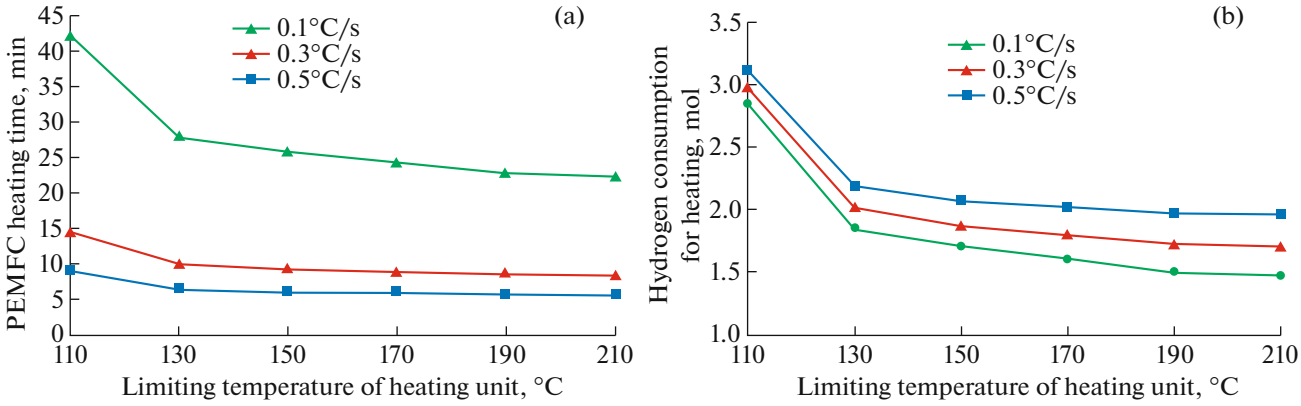

Fig. 5. (Color online) Dependence of hydrogen consumption for heating (a) and heating time of PEMFC (b) on the limiting temperature of the heating unit at different values of temperature gradients.

heating rate from the fuel cell temperature. This dependence is shown in Fig. 4a. It is clear that the temperature of the heating unit grew at a faster pace and reached a plateau with a temperature of about 150°C, which ensured the safety of the installation as a whole. In addition, in [19], an additional thermal control unit with heating and cooling circuits was used to maintain a safe temperature of the fuel plant, which leads to additional economic and energy costs.

Also important is the relationship between the given gradient and the real gradient of the FC temperature rise. The dependence of the relative gradient at different specified gradients of the temperature growth rate is shown in Fig. 4b. As can be seen from this, the real gradient of temperature growth changed in the process of fuel cell heating, but at the same time it was at a slightly lower value compared to a given gradient (at 0.5°C/s, the relative temperature rise gradient was 0.72, which means that the actual temperature rise gradient was 0.36°C/s), which ensured the unconditional preservation of the FC operability. At the same time, [35] showed that during an exothermic catalytic reaction, the temperature rise is usually at the same level of the heating rate (approximately at the level of 0.1°C/s).

The influence of the limiting temperature of the heating unit on the main characteristics of the heating process, such as hydrogen consumption and heating time, are shown in Fig. 5. As follows from the calculated data, with an increase in the range of the limiting temperature of the heating unit from 110 to 210°C both the hydrogen consumption and the heating time decreased at all values of the temperature gradient.

CONCLUSIONS

A model has been developed and a scenario for the start-up of a power plant with PEMFC with a capacity of up to 1 kW is proposed for conditions of negative temperatures in the Arctic. The obtained result was ensured by using a recombiner with a nanostructured

catalyst, which heats the internal volume of the fuel cell with air heated by the exothermic reaction of interaction of hydrogen and oxygen. The developed dynamic model showed the possibility of a successful start-up of the power plant in an autonomous mode at an ambient temperature of –50°C. The novelty of the proposed startup scenario is the use of methanol in a bubbler as an air dryer and a humidifier for reagent gases, which made it possible to significantly reduce the temperature of the start of fuel cell heating, while simultaneously ensuring the required degree of membrane moisture and fuel cell operation efficiency. The power plant and catalyst of the heating unit are protected by RF patents [32, 33].

A model study of an installation with PEMFC showed that with an increase in the heating rate of FC, the heating time decreases from 23 to 6 min, but the volume of the heating unit and the hydrogen consumption increase, however, all these parameters are lower than for analogs presented in the literature. Together however, the actual gradient of the fuel cell temperature rise did not exceed the calculated value of the fuel cell heating rate set in the model, and the temperature of the heating unit for all scenarios considered in the model reached a constant level, which ensured the safety of the installation and the fuel cell itself from overheating and destruction.

The optimal value of the specified gradient of temperature growth was 0.5°C/s because this parameter had practically no effect on the heat distribution between the FC components and reagents, however, it significantly accelerated the fuel cell heating process to ~6 min, which is currently the minimum value when compared with the literature data and reflects the originality of the results. In this case, the hydrogen consumption for heating is equivalent to several minutes of FC operation at the nominal mode.

FUNDING

This work was supported by the Russian Foundation for Basic Research (project no. 18-29-23030) and within the framework of scientific research at the NRC Kurchatov Institute (order no. 1808).

REFERENCES

1. S. I. Kozlov and V. N. Fateev, Transp. Al'tern. Topl., No. 2 (38), 7 (2014).
2. R. C. McDonald, C. K. Mittelsteadt, and E. L. Thompson, Fuel Cells, No. 3, **208** (2004). https://doi.org/10.1002/fuce.200400015
3. Q. Yan, H. Toghiani, Y. Lee, et al., J. Power Sources **160**, 1242 (2006). https://doi.org/10.1016/j.jpowsour.2006.02.075
4. M. Cappadonia, J. W. Erning, and U. Stimming, J. Electroanal. Chem. **376**, 189 (1994). https://doi.org/10.1016/0022-0728(94)03586-5
5. M. Sliwinska-Bartkowiak, J. Gras, and R. Sikorski, Langmuir **15**, 6060 (1999). https://doi.org/10.1021/la9814642
6. M. Sliwinska-Bartkowiak, G. Dudziak, R. Sikorski, et al., Phys. Chem. Chem. Phys. **3**, 1179 (2001). https://doi.org/10.1039/B009792F
7. J. Hou, H. Yu, B. Yi, et al., Electrochem. Solid-State Lett. **10**, 11 (2007). https://doi.org/10.1149/1.2363952
8. M. Khandelwal, S. Lee, and M. M. Mench, J. Power Sources **172**, 816 (2007). https://doi.org/10.1016/j.jpowsour.2007.05.028
9. R. Lin, Y. Weng, X. Lin, et al., Int. J. Hydrogen Energy **39**, 18369 (2014). https://doi.org/10.1016/j.ijhydene.2014.09.065
10. Q. Guo, Y. Luo, and K. Jiao, Int. J. Hydrogen Energy **38**, 1004 (2014). https://doi.org/10.1016/j.ijhydene.2012.10.067
11. Y. Tabe, M. Saito, K. Fukui, et al., J. Power Sources **208**, 366 (2012). https://doi.org/10.1016/j.jpowsour.2012.02.052
12. Z. Wan, H. Chang, S. Shu, et al., Energies **7**, 3179 (2014). https://doi.org/10.3390/en7053179
13. L. Yao, J. Peng, J. Zhang, et al., Int. J. Hydrogen Energy **43**, 15505 (2018). https://doi.org/10.1016/j.ijhydene.2018.06.112
14. A. Amamou, S. Kelouwani, L. Boulon, et al., IEEE Access. **4**, 4989 (2016). https://doi.org/10.1109/ACCESS.2016.2597058
15. W. S. Wheat, M. A. Meltser, and D. A. Masten, US Patent No. 8288049 B2 (2012).
16. Y. Zhou, Y. Luo, S. Yu, et al., J. Power Sources **247**, 738 (2014). https://doi.org/10.1016/j.jpowsour.2013.09.023
17. Y. Li, S. Xu, Z. Yang, et al., in *Proceedings of the International Conference on Electric Information and Control Engineering, 2011,* p. 5. https://doi.org/10.1109/ICEICE.2011.5776891
18. N. Henao, S. Kelouwani, K. Agbossou, et al., J. Power Sources **220**, 31 (2012). https://doi.org/10.1016/j.jpowsour.2012.07.088
19. J. Hwang, Appl. Energy **108**, 184 (2013). https://doi.org/10.1016/j.apenergy.2013.03.025
20. F. Knorr, D. Garcia, J. Schirmer, et al., Appl. Energy **238**, 1 (2019). https://doi.org/10.1016/j.apenergy.2019.01.036
21. T. F. Fuller and D. J. Wheeler, US Patent No. 6103410 (2000).
22. A. Amamou, M. Kidayeni, L. Boulon, et al., Appl. Energy **216**, 21 (2018). https://doi.org/10.1016/j.apenergy.2018.02.071
23. M. Sundaresan, *A Thermal Model to Evaluate Sub-Freezing Startup for a Direct Hydrogen Hybrid Fuel Cell*

Vehicle Polymer Electrolyte Fuel Cell Stack and System (Univ. of California, USA, 2004).

24. S. Surampudi, S. R. Narayanan, E. Vamos, et al., US Patent No. 5599638 (1997).
25. A. Kindler, S. R. Narayanan, and T. I. Valdez, US Patent No. 6440594 B1 (2002).
26. A. Heinzel and V. M. Barragan, J. Power Sources **84**, 70 (1999). https://doi.org/10.1016/S0378-7753(99)00302-X
27. S. Wasmus and A. Küver, J. Electroanal. Chem. **461**, 14 (1999). https://doi.org/10.1016/s0022-0728(98)00197-1
28. A. Christen and J. T. Mueller, US Patent No. 6743538 B2 (2004).
29. T. Tang, S. Heinke, A. Thuring, et al., Int. J. Hydrogen Energy **30**, 1 (2017). https://doi.org/10.1016/j.ijhydene.2017.03.236
30. H. Meng and B. Ruan, Int. J. Energy Res. **35**, 2 (2011). https://doi.org/10.1002/er
31. H. Meng, J. Power Sources **178**, 141 (2008). https://doi.org/10.1016/j.jpowsour.2007.12.035
32. G. N. Voloshchenko, V. N. Fateev, and N. A. Ivanova, RF Patent No. 194638 U1 (2019)
33. V. N. Fateev, G. N. Voloshchenko, and N. A. Ivanova, RF Patent No. 2722751 U1 (2020).
34. D. D. Spasov, N. A. Ivanova, A. S. Pushkarev, et al., Catalysts **9**, 1 (2019). https://doi.org/10.3390/catal9100803
35. S. Sun, H. Yu, J. Hou, et al., J. Power Sources **177**, 137 (2008). https://doi.org/10.1016/j.jpowsour.2007.11.012